Adsorption Behavior of Arsenate at Transition Metal Cations Captured by Amino-Functionalized Mesoporous Silicas

Hideaki Yoshitake,*,† Toshiyuki Yokoi,†,‡ and Takashi Tatsumi‡

Graduate School of Environment and Information Sciences, and Division of Materials Science and Chemical Engineering, Graduate School of Engineering, Yokohama National University, Yokohama 240-8501, Japan

Received December 17, 2002. Revised Manuscript Received February 25, 2003

We show that Fe^{3+}, Co^{2+}, Ni^{2+}, and Cu^{2+} fixed by diamino-functionalized MCM-41 and MCM-48 work as adsorption centers for arsenate ions. The stoichiometry of the N/metal cation was determined as well as the As/metal cation for the adsorption of arsenate. The effectiveness of the removal of arsenate from a dilute solution is ordered according to $Fe^{3+} > H^+ \sim Co^{2+} > Ni^{2+} \sim Cu^{2+}$, which is slightly different from the adsorption capacity: $Fe^{3+} > Co^{2+} \sim H^+ > Ni^{2+} > Cu^{2+}$. The distribution coefficients, K_d, exceed 200 000 at [arsenate] < 100 ppm in Fe/NN-MCM-41. The Fe center binds nearly three arsenate ions, which allows the adsorption capacity of Fe/NN-MCM-48 to be one of the largest at 2.5 mmol (g of adsorbent)$^{-1}$ among the adsorbents of arsenate. The difference between the meso-framework structures appears in their adsorption capacity; cation/NN-MCM-48 adsorbs a larger amount of arsenate than cation/NN-MCM-41. This is mainly caused by the difference of cation content in these functionalized mesoporous silicas. A sudden decrease in K_d for Fe/NN-MCM-41 at a coverage around $\theta = 0.3$ suggests a difference in the stabilization constant between the first and the second arsenates while $K_d(\theta)$ in Ni and Cu/NN-MCM-41 decreased gradually. The equilibrium constants, b ($=k_a/k_d$), were plotted against the coverage (Langmuir plots), where Fe^{3+} showed a minimum at $\theta = 0.65$ while b in the Ni^{2+} and Cu^{2+} sites was almost constant. The inhibition by coexisting anions such as SO_4^{2-} and Cl^- was evaluated by the suppression of the adsorption capacity. Differences between the suppression among the cations were found. We analyzed the local structure of the adsorption centers in Fe and Co captured in NN-MCM-41 by EXAFS spectroscopy.

Introduction

The synthesis and application of mesoporous molecular silicas have received considerable attention for a decade. Some of these materials, such as MCM-41[1], MCM-48,[1] FSM-16,[2] and SBA-1,[3] exhibit remarkable periodicities in their mesopore channels, large BET surface areas, high porosities, and narrow distributions of the pore size which are controllable by choosing structural directing agents.[4−7] MCM-41 and FSM-16 have a honeycomb structure (*p*6*m*, 2D hexagonal) while the pore connections of MCM-48 and SBA-1 are *Ia*3*d* and *Pm*3*n*, respectively, which are both categorized into cubic symmetry. The variation of defined framework structures has offered wide applications of these molecular sieves in heterogeneous catalysis,[8−11] gas separations,[12] and the adsorption of hazardous materials.[13−17]

The surface of mesoporous silica is considered to be covered with silanol groups whose concentration has

* Corresponding author. Address: Graduate School of Environment and Information Sciences, Yokohama National University, 79-7 Tokiwadai, Hodogaya-ku, Yokohama 240-8501, Japan. Tel: +81-45-339-4359. Fax: +81-45-339-4378. E-mail: yos@ynu.ac.jp.

† Graduate School of Environment and Information Sciences.

‡ Division of Materials Science and Chemical Engineering, Graduate School of Engineering.

(1) (a) Beck, J. S.; Vartuli, J. C.; Roth, W. J.; Leonowicz, M. E.; T. Kresge, C.; Schmitt, K. D.; Chu, C. T.-W.; Olson, D. H.; Sheppard, E. W.; McCullen, S. B.; Higgins, J. B.; Schlenker, J. L. *J. Am. Chem. Soc.* **1992**, *114*, 10834. (b) Kresge, C. T.; Leonovicz, M. E.; Roth, W. J.; Vartuli, J. C.; Beck, J. S. *Nature* **1992**, *710*, 359.

(2) Yanagisawa, T.; Shimizu, T.; Kuroda, K.; Kato, C. *Bull. Chem. Soc. Jpn.* **1990**, *63*, 988.

(3) Huo, Q.; Magolese, D. I.; Ciesla, U.; Feng, P.; Gier, T. E.; Sieger, P.; Leon, R.; Peetroff, P. M.; Schuth, F.; Stucky, G. D. *Nature* **1994**, *368*, 317.

(4) Corma, A. *Chem. Rev.* **1997**, *97*, 2373.

(5) Moller, K.; Bein, T. *Chem. Mater.* **1998**, *10*, 2950.

(6) Ying, J. Y.; Mehnert, C. P.; Wong, M. S. *Angew. Chem., Int. Ed.* **1999**, *38*, 56.

(7) Barton, T. J.; Bull, L. M.; Klemperer, W. G.; Loy, D. A.; McEnaney, B.; Misono, M.; Monson, P. A.; Pez, G.; Scherer, G. W.; Vartuli, J. C.; Yaghi, O. M. *Chem. Mater.* **1999**, *11*, 2633.

(8) Maschmeyer, T.; Rey, F.; Sankar, G.; Thomas, J. M. *Nature* **1995**, *378*, 159.

(9) Krishna, R. M.; Prakash, A. M.; Kevan, L. *J. Phys. Chem. B* **2000**, *104*, 1796.

(10) Xu, Y.; Langford, C. H. *J. Phys. Chem. B* **1997**, *101*, 3115.

(11) Hartmann, P. A.; Kevan, L. *J. Phys. Chem.* **1996**, *100*, 9906.

(12) Raimondo, M.; Perez, G.; Sinibaldi, M.; De Stefanis, A.; Tomlinson, A. A. G. *Chem. Commun.* **1997**, 1343.

(13) Kisler, J. M.; Dahler, A.; Stevens, G. W.; O'Connor, A. J. *Microporous Mesoporous Mater.* **2001**, *44*−*45*, 769.

(14) Feng, X.; Fryxell, G. E.; Wang, L.-Q.; Kim, A. Y.; Liu, J.; Kemner, K. M. *Science* **1997**, *276*, 923.

(15) Mercier, L.; Pinnavaia, T. J. *Environ. Sci. Technol.* **1998**, *32*, 2749.

(16) Noonery, R. I.; Kalyanaraman, M.; Kennedy, G.; Maginn, E. J. *Langmuir* **2001**, *17*, 528.

(17) Fryxell, G. E.; Liu, J.; Hauser, T. A.; Nie, Z.; Ferris, K. F.; Mattigod, S.; Gong, M.; Hallen, R. T. *Chem. Mater.* **1999**, *11*, 2148.

10.1021/cm0218007 CCC: $25.00
Published on Web 03/28/2003

been reported 1.2−3.0/nm^2 for MCM-41.[18−21] The high density of reactive silanols has stimulated research on a wide variety of modifications of the pore wall surfaces by the grafting of silanes. Many of the applications have been based on planting a variety of functional groups on the channel walls for controlling the molecular (or ion)−surface interactions in the pores. Divalent cations of Cu, Zn, Cr, and Ni in water were observed to be adsorbed on amino-functionalized SBA-15 more than on a thiol-functionalized form, while Hg^{2+} was preferably adsorbed on the latter.[22] SBA-15 without functionalization showed any adsorption capacity to none of these cations. The adsorption of mercury on thiol-functionalized mesoporous silicas has been intensively studied, probably due to its potential in an area of general environmental concern.[14−16,23] It has been reported that a layer of Si−$CH_2CH_2CH_2SH$ forms on MCM-41 through grafting in which the adsorption of Hg^{2+} occurs by bridging neighboring sulfur atoms with a Hg−O−Hg unit.[14] The strong point of this strategy might be the synthetic adsorption site with a molecular nature for which the adsorption capacity can be estimated basically by a certain stoichiometry. The capture of toxic ions can be designed in a similar way to the syntheses of metal-coordinated functionalized mesoporous silicas on which a number of works were published.[24−29] On the other hand, it has been demonstrated that the ratio of Hg to S depended on the kind of mesoporous silica.[15] Although this was explained by a lack of uniformity in the structure of the functional groups, an explicit investigation of the variation of the silane structures has rarely been published. The problem of the stoichiometry is important in designing the adsorbent because the uptake of the pollutant ions is, approximately, the product of surface area, the surface density of adsorption site, and the stoichiometry of the ion/site.

Recent environmental regulations in many countries have been established to control the maximum contaminant level for arsenic in drinking water to be 0.01 mg dm^{-3} (=10 ppb), as levels beyond this concentration in well water supplies has been reported as a health hazard in Bangladesh,[30] Taiwan,[31] and elsewhere.[32] The removal by adsorption has attracted a great interest in the remediation of arsenic contaminants.[33−37] Recently, it has been reported that copper(II)-coordinated ethylenediamine-functionalized MCM-41 adsorbs arsenate effectively.[17]

Since the functionalized MCM silica has an adsorption site with a molecular nature in a well-defined mesoframework structure, it is expected that we will obtain the adsorbents with a high adsorption capacity as well as insights into the mode of adsorption and the structural requirements for effective adsorption sites. In this sense, it is necessary to investigate adsorption properties at low ion concentrations as well as the adsorption saturation to clarify the stoichiometric relationship between arsenic adsorbed, the cation captured, and nitrogen (of the amino group). The inhibition effects of other anions widely found in the hydrosphere is another important factor in evaluating applicability in the environmental usage. SO_4^{2-} and Cl^- are two typical examples that are commonly found in the environment. We have already demonstrated that a complete arsenate removal by triamino-functionalized SBA-1[38,39] can be obtained. In this paper, we have investigated the adsorption properties of cation-anchored functionalized mesoporous silicas by comparing (1) two types of mesoporous framework structure, MCM-41 and MCM-48, (2) the cation centers, Fe^{3+}, Co^{2+}, Ni^{2+}, Cu^{2+}, and H^+, (3) the number of amino groups in the organic chain, and (3) the suppressions in the uptake of arsenate by coexisting sulfate and chlorate. The adsorption was evaluated mainly by the distribution coefficient, the desorption/adsorption rate constants, and the stoichiometry at the adsorption saturations. The structure of the sites showing a strong adsorption feature was analyzed by EXAFS spectroscopy.

Methods

Chemicals. Tetraethyl orthosilicate (TEOS, reagent-grade), dodecyltrimethylammonium chloride (DTMACl, >98%), and cetyltrimethylammonium chloride (CTMACl) were purchased from Tokyo Kasei Co., Ltd. Reagent-grade trimethylammonium hydroxide (TMAOH, Aldrich) and cetyltrimethylammonium hydroxide (CTMAOH, Aldrich) were used as received. 3-Aminopropyltrimethoxysilane ($H_2NCH_2CH_2CH_2Si(OCH_3)_3$) and *N*-[3-(trimethoxysilyl)propyl]ethylenediamine ($H_2NCH_2CH_2NHCH_2CH_2CH_2Si(OCH_3)_3$) were purchased from Tokyo Kasei Kogyo Co., Ltd. Their purities were >98% and >95%, respectively. N^1-[3-(Trimethoxysilyl)propyl]diethylenetriamine ($H_2NCH_2CH_2HNCH_2CH_2NH\ CH_2CH_2CH_2Si(OCH_3)_3$) was obtained from Aldrich. Potassium arsenate (KH_2AsO_4, Pr.G.) was a product of Wako Pure Chemical Industries, Ltd.

Preparation of Mesoporous Silicas. TEOS, DTMACl, and TMAOH were mixed in water and the solution was stirred for 4 h at room temperature. The composition of the gel mixture was Si:CTMACl:TMAOH:H_2O = 1:0.6:0.3:60. The gel was transferred into a Teflon bottle in an oven at 373 K. After 10 days, white precipitates were filtered and dried at 393 K. This as-synthesized powder was heated in a convex oven, where the temperature rose at 1 K min^{-1} until 903 K and remained constant for 4 h to obtain MCM-41. CTMACl and CTMAOH were used instead of DTMACl and TMAOH for

(18) Llewellyn, P. L.; Schuth, F.; Grillet, Y.; Rouquerol, F.; Rouquerol, J.; Unger, K. K. *Langmuir* **1995**, *11*, 574.
(19) Jaroniec, C. P.; Kruk, M.; Jaroniec. M.; Sayari, A *J. Phys. Chem. B* **1998**, *102*, 5503.
(20) Zhao, X. S.; Lu, G. Q. *J. Phys. Chem. B* **1998**, *102*, 1556.
(21) Zhao, X. S.; Lu, G. Q.; Whittaker, A. K.; Miller, G. J.; Zhu, H. Y. *J. Phys. Chem. B* **1997**, *101*, 6525.
(22) Liu, A. M.; Hidajat, K.; Kawi, S.; Zhao, D. Y. *Chem. Commun.* **2000**, 1145.
(23) Brown, J.; Richer, R.; Mercier, L. *Microporous Mesoporous Mater.* **2000**, *37*, 41.
(24) Holland, B. T.; Walkup, C.; Stein, A. *J. Phys. Chem. B* **1998**, *102*, 4301.
(25) Sutra, P.; Brunel, D. *Chem. Commun.* **1996**, 2485.
(26) Lau, S. H.; Caps, V.; Yeung, K. W.; Wong, K. Y.; Tsang, S. C. *Microporous Mesoporous Mater.* **1999**, *32*, 279.
(27) Evans, J.; Zaki, A. B.; El-Sheikh, M. Y.; El-Safty, S. A. *J. Phys. Chem. B* **2000**, *104*, 10271.
(28) Diaz, J. F.; Balkus, K. J., Jr. *Chem. Mater.* **1997**, *9*, 61.
(29) Park, D. H.; Park, S. S.; Choe, S. J. *Bull. Korean Chem. Soc.* **1999**, *20*, 291.
(30) Nickson, R.; McArthur, J.; Burgess, W.; Ahmed, K. M.; Ravenscroft, P.; Rahman, M. *Nature* **1998**, *395*, 338.
(31) Chen, S. L.; Dzeng, S. R.; Yang, M. H.; Chiu, K. H.; Shieh, G. M.; Wai, C. M. *Environ. Sci. Technol.* **1994**, *28*, 877.
(32) Cullen, W. R.; Reimer, K. J. *Chem. Rev.* **1989**, *89*, 713.
(33) Su, C.; Puls, R. *Environ. Sci. Technol.* **2001**, *35*, 1487.
(34) Lin, T. F.; Wu, J. K. *Water Res.* **2001**, *35*, 2049.
(35) Meng, X.; Bang, S.; Korfiatis, G. P. *Water Res.* **2000**, *34*, 1255.
(36) Wasay, S. A.; Haron, M. J.; Uchiumi, A.; Tokunaga, S. *Water Res.* **1996**, *30*, 1143.
(37) Elizalde-González, M.; Mattusch, J.; Wennrich, R.; Morgenstern, P. *Microporous Mesoporous Mater.* **2001**, *46*, 277.
(38) Yoshitake, H.; Yokoi, T.; Tatsumi, T. *Chem. Lett.* **2002**, 586.
(39) Yoshitake, H.; Yokoi, T.; Tatsumi, T. *Chem. Mater.* **2002**, *14*, 4603.

preparing MCM-48, where the gel composition was Si:CTMACl:CTMAOH:H_2O = 1:0.7:0.3:46.5. The addition of an aqueous solution of CTMAOH and CTMACl to TEOS was carried out at room temperature. The gel was heated in a Teflon bottle at 373 K for 10 days. The precipitates were filtered, washed by ethanol, and dried at 373 K. The powder was calcined at 813 K for 6 h. (The temperature increased at 1 K min^{-1} untill 813 K.)

Functionalization by Aminosilanes and Anchoring Cations. These mesoporous silicas were dehydrated at 423 K in a vacuum to remove water molecules adsorbed on the surface and were then stirred vigorously in toluene containing one monolayer equivalent amount (1.0/1 nm^2) of 3-aminopropyltrimethoxysilane, *N*-[3-(trimethoxysilyl)propyl]-ethylenediamine, or N^1-[3-(trimethoxysilyl)propyl] diethylenetriamine. These solutions were heated to 383 K in dry nitrogen for 6 h. The powder was collected by filtration, washed with 2-propanol for 2 h, and dried at 373 K. Then, 100 mg of the powder was stirred in 100 mL of 0.1 M HCl for 6 h without heating. This process converts amino groups into ammonium salts. These mono-, di-, and triamino-functionalized silica chlorides are denoted by H/N−, H/NN−, and H/NNN−mesoporous silicas, respectively, where mesoporous silica is MCM-41 or MCM-48. The amino-functionalized mesoporous silicas were alternatively treated with 0.1 M 2-propanol solution of $FeCl_3$, $CoCl_2$, $NiCl_2$, or $CuCl_2$. The amino-functionalized silica powders were stirred in the chloride solutions at room temperature for 2 h, washed two times with 2-propanol, and dried in an oven. These cation-anchored silicas are denoted as Fe/NN−MCM-41, Co/NN−MCM-48, and so forth.

Characterization and Adsorption Experiment. The mesostructural order of all powders was checked by X-ray diffraction (XRD, XL Labo, MAC Science Co., Ltd.) with Cu Kα radiation and nitrogen adsorption−desorption by BELSORP 28SA (BEL Japan Inc.). Nitrogen adsorption−desorption isotherms at 77 K were recorded using a BELSORP 28SA (BEL Japan Inc.) after the sample was evacuated at 473 K for 2 h. The surface area was evaluated by the BET method in P/P_0 = 0.05−0.25. BJH distributions were applied to determine the pore size.

The standard procedure of adsorption experiments was as follows. A 50-mg quantity of the modified mesoporous silicas were stirred for 10 h in 100 mL of aqueous solution of KH_2AsO_4. The solution was filtered to remove the solids and analyzed by induced coupled plasma (ICP) spectrometry. A typical pH value of the solution at the beginning was 6 and, after the adsorption, it decreased by ca. 3, depending on the initial concentration of arsenate. In these pH conditions, the dominant arsenate species in the aqueous solution is $H_2AsO_4^-$.[34,35]

X-ray absorption spectra of the Fe, Co, and As K edges were recorded on a BL-10B of the Photon Factory, High Energy Accelerator Research Organization, Tsukuba, Japan (Proposal #2001G133), with a ring energy of 2.5 GeV and a stored current of around 300−450 mA. A Si(311) channel cut monochromator was used. A conventional transmission mode with detection using gas ion chambers was employed. The EXAFS spectra was acquired five times under the same measuring conditions, and from the extracted spectra, the average $\chi(k)$ was calculated. The XAFS data were processed by a REX 2000 (Rigaku Co.) program assembly. The EXAFS oscillation is extracted by fitting a cubic spline function through the postedge region. After normalization using the McMaster tables, the k^3-weighted EXAFS oscillation, $k^3\chi(k)$, in the 35−130 nm^{-1} region was Fourier-transformed into a radial distribution function. The amplitudes and phase-shift functions for Fe−N, Fe−Cl, Fe−As, Co−N, Co−Cl, Co−As, and As−O bonds were calculated by FEFF 7.02 code. The curve-fitting analysis was carried out between 40 and 120 nm^{-1} in the *k*-space of inversely Fourier-transformed spectra (from FT filtered at 0.061 < *r* < 0.360 nm and 0.061< *r* < 0.320 nm for Fe K (or Co K) and As K-edges, respectively).

Table 1. BET Surface Area, Pore Size, C/N Molar Ratio, Loadings of Nitrogen and Cation, and Stoichiometry of N to Cations in Ethylenediamine-Modified Mesoporous Silicas

silica	cation	S_{BET} (m^2 g^{-1})	2 R_P (nm)	N content (mmol g^{-1})	M content (mmol g^{-1})	N/M
NN-MCM-41		586	2.63	2.76		
	Fe	310	2.24	2.09	0.55	3.8
	Co	580	2.29	1.99	0.60	3.3
	Ni	284	2.20	1.17	2.13	0.55
	Cu	588	2.32	1.89	0.53	3.6
NN-MCM-48		894	2.70	2.71		
	Fe	352	2.42	2.08	0.77	2.7
	Co	634	2.62	1.92	0.83	2.3
	Ni	305	2.40	1.08	2.7	0.40
	Cu	635	2.62	1.90	0.79	2.4

Results and Discussions

Synthesis of Cation-Incorporated Functionalized MCM Silicas. We checked the XRD patterns of the mesoporous silicas at every stage of the sample preparation. The intensity of the peaks decreased while their positions were not changed by silylation and cation coordination, suggesting that the meso-framework structures were basically retained. The change in XRD patterns due to the grafting, cation incorporation, and arsenate adsorption is discussed below.

Table 1 summarizes the results of nitrogen adsorption experiments (BET surface area and most probable pore diameter in BJH distributions) and elemental analysis (nitrogen and cation contents and N/M stoichiometry) of M/NN-mesoporous silicas. The structural parameters in NN-mesoporous silicas are also listed for comparison. It is to be noted that the surface area decreases as S_{BET}(Co) = S_{BET}(Cu) > S_{BET}(Fe) > S_{BET}(Ni). The pore sizes were decreased by cation coordinations, suggesting that a thickening of the walls occurred in all the cation−silica pairs. The N content of Ni-MCM is clearly lower than that of the other cations and the N/M ratio for Ni is far below unity. This stoichiometry demonstrates that the Ni^{2+} is occluded into NN-mesoporous silicas beyond the coordination with amino groups. The adsorption of nickel actually occurred on unfunctionalized mesoporous silicas and, consequently, the homogeneity of the adsorption sites in Ni/NN-mesoporous silicas is very doubtful. Despite the difference of surface area, the N content was calculated to be 1.99 ± 0.10 mmol g^{-1} for all M/NN-MCM-41 and M/NN-MCM-48 except Ni/NN-mesoporous silicas. Assuming that the charge of metal cations are neutralized by chloride in calculating the weight gain by anchoring Fe^{3+}, Co^{2+}, and Cu^{2+}, the decrease of N content reveals that the 14−22% of fixed silane is lost during the cation coordination. The N/M ratio is influenced by the coordination structure of the cations. Fe/NN-MCM-41 and Cu/NN-MCM-41 approximately follow M:en = 1:2 while the mixture of 1:1- and 1:2-coordinated structures explains well the N/M of Co/NN-MCM-41. The notable difference between MCM-41 and MCM-48 is found in the cation content. The ethylenediamine groups in NN-MCM-48 bound more metals than NN-MCM-41, suggesting that the 1:2 coordinations of en to Fe, Co, and Cu cations are fewer in MCM-48 than in MCM-41. Considering that N/M also depends on the molecular structure of the silane shown below (Table 3), it is probable that N/M is sensitive to the density of the amino group, the configuration of the

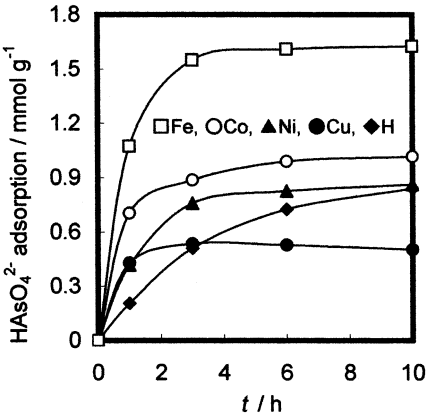

Figure 1. Time evolution of the adsorption of arsenate by M /NN-MCM-48 where M = Fe (□), Co (○), Ni (▲), Cu (●), and H (◆). 12.2 mmol/L of $HAsO_4^{2-}$ and 50 mg of adsorbent were mixed in 10 mL of water. The reaction time was 10 h and the reaction temperature 298 K.

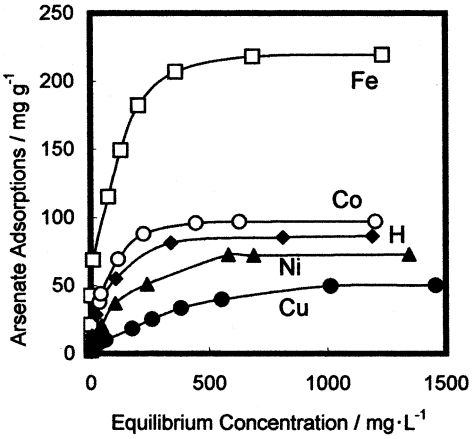

Figure 2. Adsorption isotherms of arsenate by M /NN-MCM-48 where M = Fe (□), Co (○), Ni (▲), Cu (●), and H (◆). Reaction conditions: 50 mg of adsorbent, 10 mL of water as a solvent, reaction time 10 h, and reaction temperature 298 K.

functional group, and the influence of the other surface groups and defects. NN-MCM-48 requires fewer amino groups to fix a cation and, consequently, captures a greater number of cations than NN-MCM-41.

Adsorption of Arsenate on Cation-Incorporated NN−MCM Silicas. Figure 1 shows the evolution of the arsenate adsorption on M/NN-MCM-48. A difference of the initial rate, r(Fe) > r(Co) > r(Ni) ∼ r(Cu) > r(H), was observed. The adsorption by the metal cations reached equilibrium at 6 h while 10 h was necessary to equilibrate the adsorption on protonated NN-MCM-48. Since significant differences were not found in the pore sizes (Table 1), the observation of the difference in the sorption rates demonstrates that the adsorption is not controlled by diffusion processes but by the affinity of the site. The result also implies that the restriction by the pore size is negligible in the removal of toxic anions by functionalized MCM-silicas.

The adsorption isotherms for cationated NN-MCM-48 are overlaid in Figure 2. When the equilibrium concentration was 800 mg L^{-1}, the adsorption was almost saturated. Fe/NN-MCM-48 showed a vertical increase until the adsorbed arsenate reached 40 mg/g of adsorbent (mg g^{-1}), where the concentration of the anion decreased to the detection limit of the ICP analysis (<1 ppb). A difference among the cations appeared in the adsorption in low-concentration regions as well as at saturation.

Table 2. Adsorption Capacity (C_{max}) and Stoichiometry of Arsenic to Cations (As/M) at the Saturation of Adsorption on M/NN-Mesoporous Silicas[a]

	Fe^{3+}		Co^{2+}		Ni^{2+}		Cu^{2+}	
	C_{max}[b]	As/M	C_{max}[b]	As/M	C_{max}[b]	As/M	C_{max}[b]	As/M
MCM-41	1.6 226	2.8	0.69 97	1.2	0.52 73	0.25	0.36 51	0.69
MCM-48	2.5 353	2.7	1.0 141	1.2	0.86 121	0.32	0.50 71	0.65

[a] Experimental conditions: adsorbent, 50 mg; water, 10 mL; reaction time, 10 h; reaction temperature, 298 K. [b] mmol·(g of adsorbent)$^{-1}$ in upper cells and mg (g of adsorbent)$^{-1}$ in lower cells.

The adsorptions on M/NN-MCM-41 followed the same patterns as in Figures 1 and 2 qualitatively.

The adsorption capacities and the stoichiometry of As to M^{n+} are summarized in Table 2. The adsorption capacity of the Fe center is larger than that of any other cations; it is 1.6−2.5 mmol (226−352 mg) per g of adsorbent, depending on the support. Large adsorption capacities of arsenate have been reported for organic−inorganic composites where the inorganic sites are dispersed on inorganic/organic supports whose density is much smaller than that of pure inorganic minerals. Values such as 0.7 mmol g^{-1} for molybdate-impregnated chitosan beads,[40] 0.5 mmol g^{-1} for copper-chelated polymers,[41] and 1.0 mmol g^{-1} for Cu/NN-MCM-41[17] are the notable examples in recent studies. The data for Fe/NN-mesoporous silica dominate adsorption capacities of all reports shown above and, to the best of our knowledge, 2.5 mmol/g of adsorbent is more than any of the adsorption capacities previously reported. The order of cations in the specific adsorption is Fe^{3+} > Co^{2+} > Ni^{2+} > Cu^{2+}, which is slightly different from the specific adsorption at low arsenate concentrations as shown in Figure 2. As for Cu/NN-MCM-41 and Cu/NN-MCM-48, about 70% of the metal works as an adsorption site if a stoichiometry of 1:1 is assumed. A significant difference in N/M was not found between M/NN-MCM-41 and M/NN-MCM-48, suggesting that the local structure of the cation anchoring sites is the same between the two mesoporous silicas and the difference in surface area influences the adsorption capacity. Since, despite the large amount occluded in NN-mesoporous silicas, a large part of the Ni^{2+} does not adsorb arsenate, we cannot discuss quantitatively the arsenate adsorption on Ni centers. Fe/NN-MCM-41 shows a stoichiometry of nearly 3:1 while the ratio becomes 2:1 in Fe/NN-MCM-48 and almost 1:1 in Co/NN-MCM-41 and NN-MCM-48 in Table 2. As arsenate is monovalent at the pH range in the adsorption equilibrium, the remaining Cl^- probably neutralizes the positive charge of the cations.

The adsorption capacity of Cu/NN-MCM-41 measured by Fryxell et al., at 1.0 mmol g^{-1},[17] is notably larger than the datum (0.36 mmol g^{-1}) in Table 1. This disagreement is likely caused by the larger number of Cu^{2+} ions anchored, 1.0−1.4 mmol g^{-1}, which is almost

(40) Dambies, L.; Guibal, E.; Roze, A. *Colloid Surf. A* **2000**, *170*, 19.
(41) Ramana, A.; Sengupta, A. K. *J. Environ. Eng.* **1992**, *118*, 755.

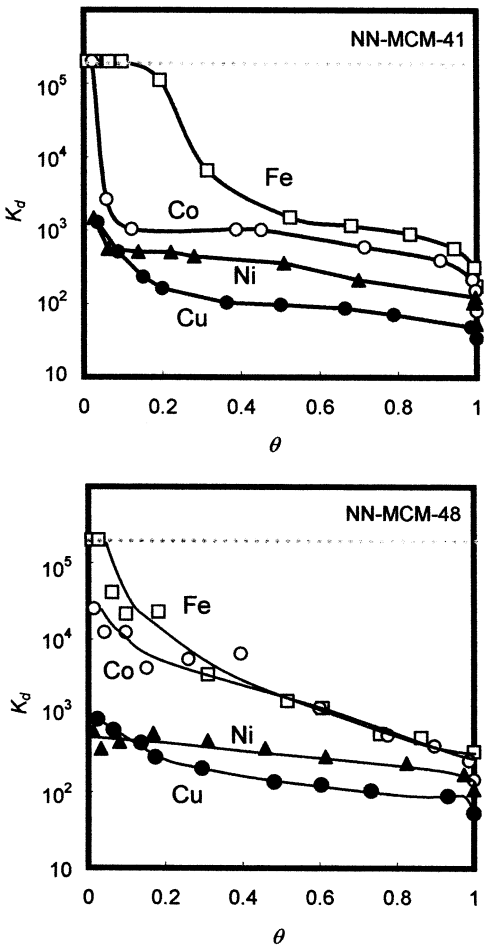

Figure 3. Distribution coefficient versus coverage of arsenate for metal-loaded NN-MCM-41 (upper) and NN-MCM-48 (lower). The broken lines show the detection limit of ICP analysis.

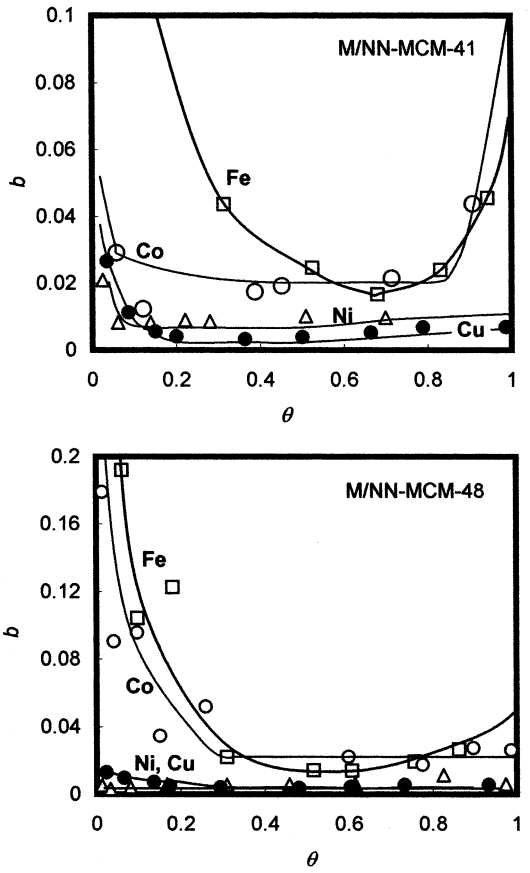

Figure 4. Equilibrium constant for adsorption as a function of the coverage of arsenate (Langmuir plots) for metal-loaded NN-MCM-41 (upper) and NN-MCM-48 (lower). Fe^{3+} (□), Co^{2+} (○), Ni^{2+} (▲), and Cu^{2+} (●).

2−3 times larger than the density in this study, 0.53 mmol g^{-1} (Table 1). The As/Cu ratio in their study, 1.0/1.4 = 0.71, shows excellent agreement with this study, 0.69 (Table 2). Thus, the difference in the capacity is explained simply by that of the loading of Cu^{2+} per unit weight of NN-MCM-41.

The adsorption capacity C_{max} is much larger in M/NN-MCM-48 than in M/NN-MCM-41 (Table 2). Since As/M and N contents are almost the same between two mesoporous silicas, the difference in C_{max} is caused by that in the N/M ratio (Table 1).

We also prepared Fe/NN-amorphous silica (Cab-O-sil M5, S_{BET} = 170 m^2 g^{-1}) for comparison. The adsorption capacity of arsenate was 0.97 mmol (g of adsorbent)$^{-1}$, where As/Fe = 1.2. The small adsorption capacity can be attributed to the surface area (S_{BET} = 117 m^2 g^{-1} after the grafting of NN-silane) and a low activity of Fe.

Assuming that arsenate covers the surface sites completely (i.e., $\theta = 1$) at the adsorption saturation, the distribution coefficient, K_d, is plotted against the coverage in Figure 3. When the initial concentration was low, the arsenate remaining in the solution after the adsorption was lower than the detection limit of ICP and K_d became more than 200 000. This complete removal was observed typically in the adsorption by Fe/NN-MCM-41. The sudden decrease of K_d at $\theta = 0.3$ for Fe/NN-MCM-41 implies the change in the mode of adsorption at this coverage. This drastic change in K_d is likely caused by the reduction of the affinity after one As is bound to Fe, considering 2.8 As are adsorbed on an Fe site at $\theta = 1$. K_d decreased again at θ = 0.7−0.8, suggesting that adsorption becomes even weaker after two arsenates are coordinated to Fe. Although at quite low coverages Co/NN-MCM-41 showed K_d >200 000, its value suddenly decreased below $\theta = 0.1$, suggesting a very small number of strong adsorption sites. At θ > 0.1, K_d gradually decreased just like Ni and Cu/NN-MCM-41. The order of K_d among the cations, Fe^{3+} > Co^{2+} > Ni^{2+} > Cu^{2+}, agrees with that for the adsorption capacity C_{max}. Such sudden decreases as were observed in Fe and Co/NN-MCM-41 were not found in M/NN-MCM-48. All cations showed a continuous decrease of K_d according to θ. The order of K_d among the cations is Fe^{3+} > Co^{2+} > Ni^{2+} > Cu^{2+}, which agrees with that for M/NN-MCM-41.

Although a large and sudden change in the affinity can be found in Figure 3, a more precise treatment is necessary to explore the adsorption characteristics dependent on the coverage because K_d is a function of the concentration of arsenate in the solution, C. For the Langmuir equation, the equilibrium constant, $b = k_a/k_d = \theta/C(1-\theta)$, where k_a and k_d are the rate constants of adsorption and desorption, respectively, and C is the concentration of arsenate in the solution, is independent of θ according to his theory. The results of adsorption isotherms were converted to b vs θ as shown in Figure 4. In the edge ranges, when θ approaches 0.1 or 0.9, b

Table 3. Stoichiometry of Nitrogen with Respect to the Cations (N/M) and Arsenic to Cations (As/M^{n+}) at the Saturation of Adsorption on M/Mono- and Triamino-functionalized Mesoporous Silicas[a]

	Fe^{3+}		Co^{2+}	
	N/M	As/M	N/M	As/M
N-MCM-41	3.1	2.1	2.5	1.1
NNN-MCM-41	2.8	1.6	7.9	1.3
N-MCM-48	2.0	1.6	1.8	1.2
NNN-MCM-48	2.8	1.4	7.0	1.1

[a] Experimental conditions: adsorbent, 50 mg; water, 10 mL; reaction time, 10 h; reaction temperature, 298 K.

apparently diverges because the precise quantification of C is difficult while θ or $1 - \theta$ linearly approaches zero and the numerical errors become large. Ni- and Cu-centered adsorbents show a constant b and the Langmuir equation therefore applies quite well. The value of b of Fe/NN-mesoporous silicas has a minimum around $\theta = 0.65$, which demonstrates that the adsorption is gradually suppressed according to θ in $\theta < 0.65$ and is enhanced with θ in $\theta > 0.65$. This discontinuity suggests the formation of a monolayer of 2As−Fe complexes and a change in mode of interactions. Around $\theta = 0.65$, b rises or stops decreasing in Co/NN-MCM-41 and Co/NN-MCM-48, respectively. This suggests a change in the mode of interactions. However, this is not attributable to the preferential formation of fewer coordinated species but to an enhancement of the desorption at the "crowded surface." The difference in the framework structures is probably related to the slight difference in the behavior of Co/NN-MCM-41 and Co/NN-MCM-48.

We further investigated the ligand effects on the adsorption of arsenate by functionalizing with mono- and triaminosilanes instead of diaminosilane. Table 3 shows the N/M ratio in the adsorbents and As/M at the adsorption saturation. The N/M stoichiometry depends both on the stability of complexes and on the surface density of functional groups. Despite showing similar N/Fe, the As/Fe of Fe on N- and NNN-mesoporous silicas was 1.4−2.1 and clearly smaller than As/Fe of Fe on NN-mesoporous silicas (2.7−2.8). On the other hand, N/Co was different among the silicas while no significant difference was found in As/Co. The As/Co ratio in mono- and diamino-functionalized MCM-41 and MCM-48 fell to between 1.1 and 1.3 in Table 3 while that for Co/NN-mesoporous silicas was 1.2. The significant decrease (by 25−43% and 41−48% for MCM-41 and MCM-48, respectively,) in the number of coordinated As to Fe^{3+} anchored by mono- and triamino-functional groups suggests that the ethylenediamine-type ligand enhances the formation of As−Fe bonds.

Inhibition of Adsorption by Cl^- and SO_4^{2-}. In the removal of arsenate in an environment, the inhibition by other anions should be considered. The suppression of the arsenate adsorption was evaluated from the adsorption capacity in the presence of the inhibiting anion divided by the adsorption capacity in the absence of the inhibiting anion. This is presented as a function of the concentration of the inhibitor anions in Figure 5. Co^{2+} showed nearly consistent adsorption capacity against Cl^- while the suppression in Fe^{3+} is ranked between those of Co^{2+} and Ni^{2+}. The suppressions for Cu^{2+} and H^+ were significantly large. In the presence

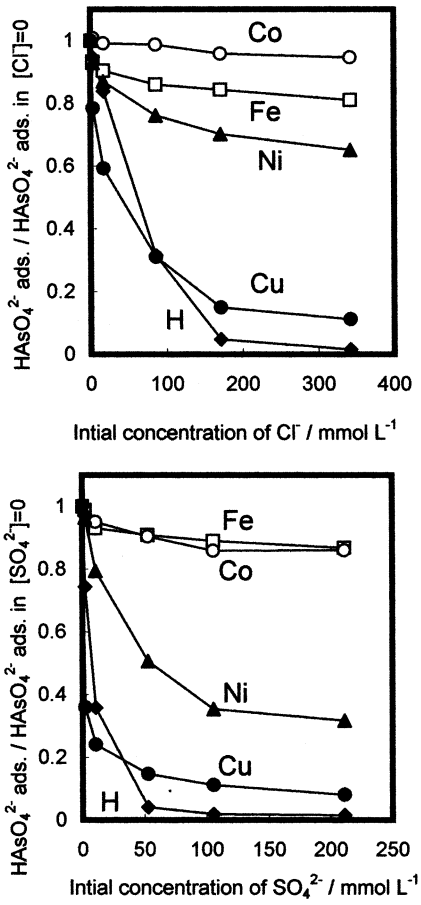

Figure 5. Suppression of the adsorption of arsenate in the coexistence of Cl^- (upper) and SO_4^{2-} (lower). The cations fixed by the ethylenediamine group were Fe^{3+} (□), Co^{2+} (○), Ni^{2+} (▲), Cu^{2+} (●), and H^+ (◆). 12.2 mmol/L of $HAsO_4^{2-}$ and 50 mg of adsorbent were mixed in 10 mL of water. The reaction time was 10 h and the reaction temperature 298 K.

of competing sulfate, arsenate adsorption by the Fe and Co/NN-MCM-41 was largely unaffected; however, the Cu^{2+}- and H^+-based systems suffered considerable inhibition. The concentration in these plots is far above typical environmental conditions. The average composition of the ions in rivers of the world is $[Cl^-] = 0.16-0.23$ and $[SO_4^{2-}] = 0.086-0.18$ mmol L^{-1}.[42,43] The function required for the adsorbents would be the selective adsorption of arsenate of several 10 ppb in these anions. The inhibition due to these above-average concentrations is observed to be negligible by extrapolation of the plots in Figure 5. In addition, the distribution coefficients in arsenate adsorptions become larger with diluting the solution. On the basis of these considerations, the adsorption characteristics of As in the environment are expected to be unchanged in the presence of SO_4^{2-} and Cl^- below the range of mmol L^{-1}.

The release of arsenate occurs more easily in H^+ sites than on M^{n+} ones so that the exchange rates due to Cl^- and SO_4^{2-} anions would be similar among all cationated NN-MCM-41 when a meaningful amount of H^+ sites exist in M/NN-MCM-41. In contrast, the absence of the rapid decrease of ($H_2AsO_4^-$ adsorption)/($H_2AsO_4^-$ adsorption in [inhibiting anion] = 0) near [inhibiting

(42) Meybeck, M. *Rev. Geol. Dyn. Geogr. Phys.* **1979**, *21*, 215.
(43) Conway, E. J. *R. Irish Acad., Proc. B* **1942**, *48*, 119.

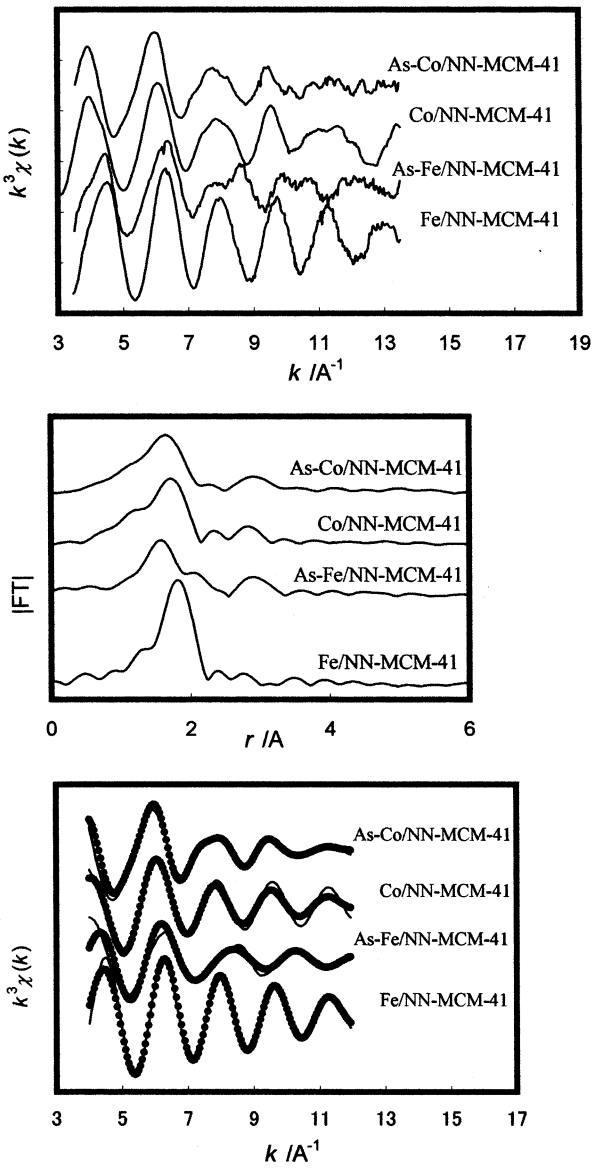

Figure 6. EXAFS oscillations, Fourier transforms, and curve-fitting results (circles: experiment; lines: theory) of Fe and Co K-edge EXAFS of Fe/NN-MCM-41 and Co/NN-MCM-41 prior to and following arsenate adsorption.

anion] = 0 in Fe, Co, and Ni sites demonstrates that the contribution of the H^+ site to the adsorption capacity in M/NN-MCM-41 (M = Fe, Co, and Ni) is negligible.

Local Structure of Fe and Co. In a homogeneous solution, tris(ethylenediamine)iron(III) sulfate has been known for an $Fe(en)_3$ complex.[44] The stability constants for the ethylenediamine ligand for Co(II) is log K_1 = 5.97, log K_2 = 4.91, and log K_3 = 3.18 (in ionic strength of 1.4 mol dm^{-3}) while that for Cu(II) is log K_1 = 10.72, log K_2 = 9.31, and log K_3 = −1.0.[45] The third constant was not able to be measured unless the concentration was high enough.[45,46] These results for the homogeneous chemistry imply that the form of 3-fold coordination by an en ligand is likely stable. It is well-known that, in d^9 octahedral complexes, the number of electrons in the e_g orbital is odd and *trans*-$[Cu(en)_2(H_2O)_2]^{2+}$ is very stable. The fixation of the silane on the surface considerably decreases the degree of freedom in the motion of en and, consequently, a high surface density (more than 3 ethylenediamines per nm^2) is necessary to obtain an $M(en)_3$ complex. In contrast, calculated surface en density (=(N content)/2S_{BET}) in Table 1 varies from 0.90 to 2.03 per nm^2. These values support that $M(en)_2Cl^-_n$ and $M(en)Cl^-_n$ are the major species on NN-MCM-41 and NN-MCM-48.

Table 4. EXAFS Curve-Fitting Results for Fe/NN-MCM-41 and Co/NN-MCM-41[a]

	shell	N	r (nm)	σ^2
	Fe K-edge			
Fe/NN-MCM-41	N	3.3(0.6)	0.192(0.03)	0.112
	Cl	2.1(0.4)	0.224(0.03)	0.062
As−Fe/NN-MCM-41	N	3.0(0.4)	0.194(0.03)	0.064
	Cl	0.4(0.2)	0.227(0.03)	0.055
	As	1.6(0.5)	0.327(0.04)	0.063
	Co K-edge			
Co/NN-MCM-41	N	3.1(0.7)	0.183(0.04)	0.091
	Cl	1.6(0.3)	0.249(0.05)	0.061
As−Co/NN-MCM-41	N	4.1(0.6)	0.184(0.03)	0.085
	Cl	0.7(0.2)	0.238 (0.04)	0.065
	As	1.2(0.3)	0.305(0.04)	0.088
	As K-edge			
As−Fe/NN-MCM-41	O	3.9(0.4)	0.169(0.03)	0.044
	Fe	0.95(0.2)	0.327(0.04)	0.058
As−Co/NN-MCM-41	O	3.8(0.5)	0.169(0.03)	0.043
	Co	1.1(0.2)	0.310(0.04)	0.069

[a] The numbers in the parentheses are the errors. *R*-factor was 1−5%.

Figure 6 shows $k^3\chi(k)$ EXAFS, radial distribution functions and the result of curve-fitting analysis of Fe and Co K-edge EXAFS of Fe/ and Co/NN-MCM-41 prior to and following arsenate adsorption. The arsenate was fully adsorbed. The EXAFS oscillation of Fe was completely changed after arsenate adsorption. Before the adsorption, a strong peak around 0.19 nm, attributed to the Fe−Cl shell, is accompanied with a shoulder peak around 0.13 nm in the Fourier transform. As shown in the result of curve-fitting analysis in Table 4, the coordination number of the Cl shell, N(Fe−Cl), was calculated to be 2.1 with the distance, r(Fe−Cl), of 0.224 nm. Coupled with the result of the N/Fe stoichiometry in Table 1, it is likely that the ligands of Fe^{3+} are 2 en and 2 Cl^-. A minor contribution of the coordination of a water molecule is possible. The small shoulder peak is assigned to the Fe−N shell, though it is generally difficult to distinguish N scatterer from O in analyzing EXAFS spectra. The coordination number and the distance are N(Fe−N) = 3.3 and r(Fe−N) = 0.192 nm, respectively. The Debye−Waller factor, σ, for this bond is 0.112, suggesting a structural disorder in en ligand coordination, which can be caused by a steric hindrance arising from the fixation on the surface, ligand exchange reactions between en groups or between en and water, and so forth. In the spectrum after the arsenate adsorption, the peak for Fe−N became larger while the intensity of the peak for Fe−Cl significantly decreased. N for Fe−N and Fe−Cl was calculated to 3.0 and 0.40, respectively. The value of σ for the former bond decreased to 0.064. A value of N below unity for Fe−Cl implies the loss of the chemical bonds. The bond length remains nearly the same, 0.194 and 0.227 nm for Fe−N and Fe−Cl, respectively. A new peak appears around

(44) Garg, A. N.; Shukla, P. N.*Indian J. Chem.* **1974**, *12*, 996.
(45) Pecsok, R. L.; Bjerrum, J. *Acta Chem. Scand.* **1957**, *11*, 1419.
(46) Gordon, G.; Birdwhistell, R. K. *J. Am. Chem. Soc.* **1959**, *81*, 3567.

0.28 nm. This is assigned to an As shell. The *R* factor was smaller than 5% in the fitting with the parameters, N(Fe−As) = 1.6 and r(Fe−As) = 0.327 nm. The coordination number supports the 2As−Fe coordination. To explain the gap between elemental analysis and N(Fe−As) in EXAFS, we propose the model where two arsenate ions are directly coordinated to Fe^{3+} and the other is bound in the outer sphere to compensate the positive charge of the ferric cation. Taken together, these results suggest that the original Fe complex is $Fe(III)(en)_2Cl^-_2$, with a third Cl^- in the outer sphere to neutralize charge. Adsorption of arsenate results in the displacement of all of these Cl^- ions, resulting in two $H_2AsO_4^-$ ions bound to the Fe center and a third in the outer sphere of the complex.

The Co K-edge EXAFS oscillation in the large k region ($k > 10$ Å^{-1}) was changed after the adsorption of arsenate. The coordination numbers before adsorption, N(Co−N) = 3.1 and N(Co−Cl) = 1.6, imply that the coordination environment of Co is composed of two en ligands and two Cl^-. The relatively large Debye−Waller factors suggest the disorder of the coordination structure. The nitrogen shell prior to and following the adsorption of arsenate agrees within the error limit. On the other hand, instead of the decrease of Co−Cl bond, Co−As appeared as N(Co−As) = 1.2 and r(Co−As) = 0.305 nm, suggesting that one arsenate coordinates to Co.

In $k^3\chi(k)$ EXAFS of As K-edge plotted in Figure 7, a new oscillation is clearly overlaid by the presence of adsorbents, Fe/NN-MCM-41 or Co/Nn-MCM-41. The new oscillation appeared as a peak at around 3.8 Å in the Fourier transform, which is attributed to As−Fe and As−Co bonds ($N = 0.95$, $r = 0.327$ nm and $N = 1.1$, $r = 0.310$ nm, respectively). The strong feature in the Fourier transforms is due to the As−O bond ($N = 3.9$, $r = 0.169$ nm and $N = 3.8$, $r = 0.169$ nm, respectively). The peak for As−O was almost unchanged from the spectrum of arsenate solution. The coordination number and bond length agree with the model of Fe bound to 2As with 0.327 nm proposed by the analysis of Fe K-edge EXAFS, which ensure the validity of the analysis. The EXAFS spectroscopy has been applied to the arsenate adsorbed on ferrihydrite[47,48] and iron (hydr)-oxides.[49,50] The adsorption on these natural iron minerals results in more than two kinds of structures. However, the most prominent peaks appeared around 0.325 nm in all of the studies. The bond length falls between the distances of monodentate (r = ca. 0.36 nm), bidentate (r = ca. 0.325 nm), and edge-shared coordinations (r = ca. 0.285 nm) of the As (T_d) and Fe (O_h) oxide complexes. Although similarities are found in the structural parameters of EXAFS analysis, the models on the iron oxides cannot be applicable to the adsorption site with a molecular nature in this study. The structural parameters for As−Co bond are in good accordance with a model proposed to Co K-edge EXAFS, where one arsenate is bound to Co. The bond length of As−Co agrees with that of Co−As, which is shorter than the Fe−As bond.

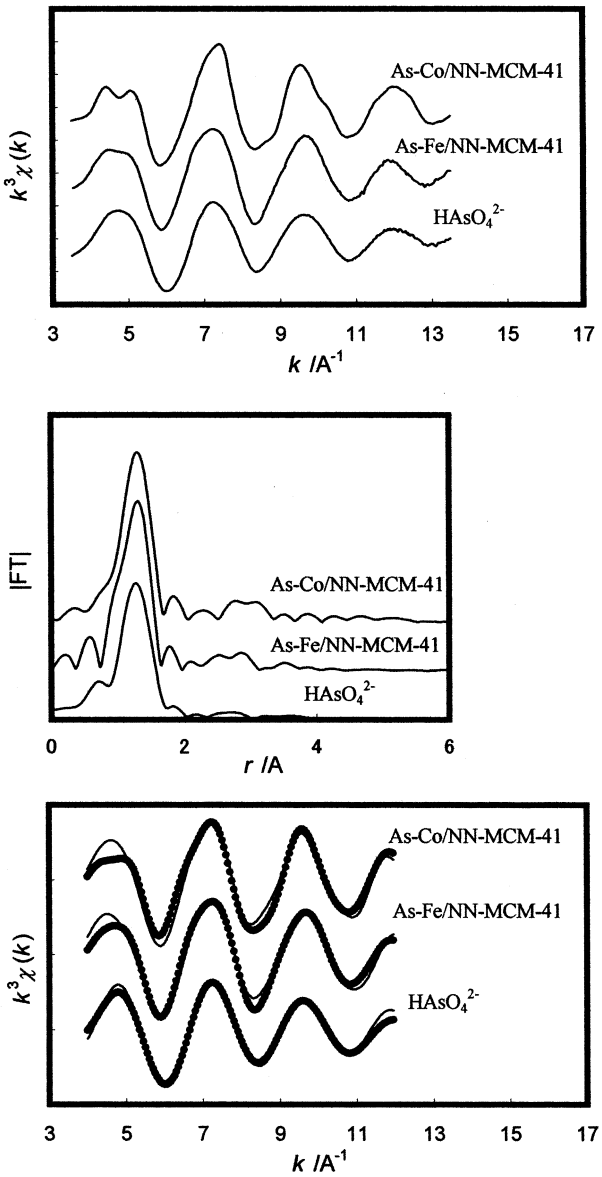

Figure 7. EXAFS oscillations, Fourier transforms, and curve-fitting results (circles: experiment; lines: theory) of As K-edge EXAFS of arsenates adsorbed on Fe/NN-MCM-41 and Co/NN-MCM-41.

The coordination numbers determined by EXAFS agrees with the stoichiometries of N/Fe, N/Co, As/Fe, and As/Co, in Tables 1 and 2. This implies that most of the amino groups are bound to Fe and Co in NN-MCM-41 and the contribution of protonated amine is small in the adsorption of arsenate.

Degradation of Framework Structure and Influence on Adsorption Capacity. The XRD patterns of adsorbents prior to and following arsenate adsorption are compared in Figure 8. The patterns of original MCM-41 and NN-MCM-41 are also shown in the figure. The (110) and (200) reflections disappeared after the grafting of diaminosilane. After the incorporation of cations, the intensity of the prominent (100) peak decreased significantly. The reduction of the intensity is the largest at this stage. The adsorption of arsenate reduced the peak intensity. The BET surface area was 1283, 586, 310, and 73 m^2 g^{-1} for MCM-41, NN-MCM-

(47) Waychunas, G. A.; Rea, B. A.; Fuller, C. C.; Davis, J. A. *Geochim. Cosmochim. Acta* **1993**, *57*, 2251.
(48) Waychunas, G. A.; Davis, J. A.; Fuller, C. C. *Geochim. Cosmochim. Acta* **1995**, *59*, 3655.
(49) Manceau, A. *Geochim. Cosmochim. Acta* **1995**, *59*, 3647.
(50) Fendorf, S.; Eick, M. J.; Grossl, P.; Sparks, D. L. *Environ. Sci. Technol.* **1997**, *31*, 315.

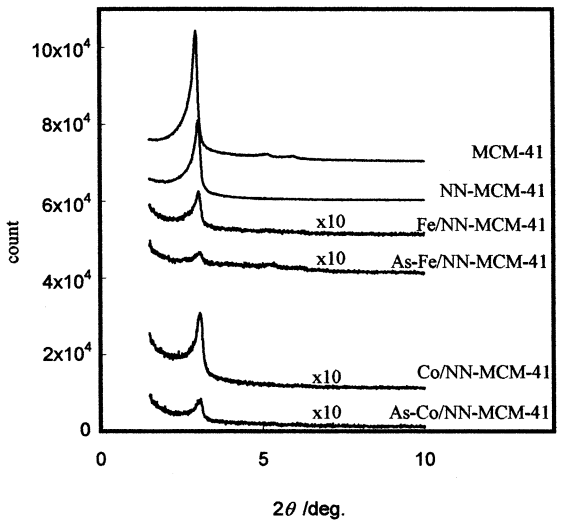

Figure 8. X-ray diffraction pattern of MCM-41 structure following grafting with diamino silane (NN-MCM-41), anchoring Fe and Co (Fe/NN-MCM-41 and Co/NN-MCM-41, respectively) and adsorbing arsenate (As−Fe/NN-MCM-41 and Co/NN-MCM-41, respectively).

41, Fe/NN-MCM-41, and As−Fe/NN-MCM-41, respectively. The degree of decrease is larger than that in Co/NN-MCM-41 and As−Co/NN-MCM-41 (384 and 193 $m^2 g^{-1}$, respectively). The reductions in intensity of XRD reflections and BET surface area suggest a destruction of the mesostructure in acidic solutions. The larger degree of structural degradation in Fe/NN-MCM-41 and As−Fe/NN-MCM-41 is explained by the smaller pH in $FeCl_3$ and arsenate solutions. (During the adsorption, Cl^- is desorbed from the adsorbent and the affinity of chloride is different between Fe^{3+} and Co^{2+}.)

The results on the mesostructure after adsorption can cause doubt on clean removal without significant leaching of cations and amines due to the decomposition of adsorption centers. In contrast, the leaching of the cation was typically 3 and 1% for Fe and Co, respectively, and the loss of nitrogen after the adsorption of arsenate was <5%. This reveals that the destruction of the mesoporous structure measured by XRD and N_2 adsorption is not related directly to the damage on the adsorption sites. The influence of structural degradation should be considered in the regeneration of used adsorbents rather than in the contamination of solution. We reactivated As−Fe/NN-MCM-41 by washing with 1 M HCl, resulting in further decrease in the peak intensity in XRD (not shown in the figure). Since this treatment removed 99.9% arsenate as well as 95% of Fe^{3+} from the used adsorbent, Fe^{3+} was incorporated again by the same procedure, as is described in the Experimental Section. The incorporation of Fe reached 76% of the fresh Fe/NN-MCM-41 and 91% of the adsorption capacity was recovered by this recycle procedure. The successful regeneration of used adsorbent reveals that the lowering of the mesoporous order accompanied by reduction of the surface area is not crucial to the function of adsorbent.

Conclusion

Transition metal cations, Fe^{3+}, Co^{2+}, Ni^{2+}, and Cu^{2+}, were captured by diamino-functionalized MCM-41 and MCM-48. The results of elemental analysis were consistent with the 2:1 and 1:1 coordinations of the en ligand to metal cations; the average forms of Fe and Cu on NN-mesoporous silicas were $Fe(en)_2$ and $Cu(en)_2$, respectively, while Co^{2+} bound to nearly one en ligand. Ni^{2+} was adsorbed on unfunctionalized mesoporous silicas, resulting in low N/ Ni^{2+}. Fe^{3+} and Co^{2+} were the central cations that were superior to the other cations in terms of (1) the complete removal of As from the solutions evaluated by K_d, (2) high adsorption capacities, and (3) adsorption selectivity in the solution with inhibiting anions such as SO_4^{2-} and Cl^-. The distribution coefficient (K_d) between solid and solution became larger than 200 000 at [arsenate] < 100 ppm for Fe/NN-MCM-41. The largest adsorption capacity of arsenate, 2.5 mmol (g of adsorbent)$^{-1}$, was achieved in Fe/NN-MCM-48, in which Fe^{3+} bound to 2.7 arsenate anions. The adsorption capacity of M/NN-MCM-48 (M = Fe, Co, Ni, Cu) is much larger than that of M/NN-MCM-41, though the As/M stoichiometries are almost the same. This is attributed to the larger cation incorporations in NN-MCM-48 than in NN-MCM-41. The comparison between metal cations and protons in the presence of inhibitor anions implied that the uncoordinated functional group is negligible or does not work in the arsenate adsorption on M/NN-mesoporous silicas. The comparison between mono-, di-, and triamino-functionalized MCM-41 suggested that the $Fe(en)_2$ structure is essential to achieving a high As/Fe ratio at the adsorption saturation. The bond formation between cations and As was confirmed by Fe, Co, and As K-edge EXAFS.

Acknowledgment. This work was partly supported by Grand-in-Aid for Scientific Research (Grant No. 13780448) from JSPS.

CM0218007